Redox Biology 68 (2023) 102945

Contents lists available at ScienceDirect

Redox Biology

journal homepage: www.elsevier.com/locate/redox

A novel combination therapy with Cabozantinib and Honokiol effectively inhibits c-Met-Nrf2-induced renal tumor growth through increased oxidative stress

Laxminarayan Rawat [a,b], Murugabaskar Balan [a,b], Yuzuru Sasamoto [a,c,d], Akash Sabarwal [a,b,1], Soumitro Pal [a,b,*,1]

[a] Division of Nephrology, Boston Children's Hospital, Boston, MA, USA
[b] Harvard Medical School, Boston, MA, USA
[c] Division of Genetics, Brigham and Women's Hospital, MA, USA
[d] Department of Ophthalmology, Boston University Chobanian & Avedisian School of Medicine, Boston, MA, USA

ARTICLE INFO

Keywords:
Renal cancer
c-Met
Nrf2
Honokiol
Oxidative stress

ABSTRACT

Receptor tyrosine kinase (RTK), c-Met, is overexpressed and hyper active in renal cell carcinoma (RCC). Most of the therapeutic agents mediate cancer cell death through increased oxidative stress. Induction of c-Met in renal cancer cells promotes the activation of redox-sensitive transcription factor Nrf2 and cytoprotective heme oxygenase-1 (HO-1), which can mediate therapeutic resistance against oxidative stress. c-Met/RTK inhibitor, Cabozantinib, has been approved for the treatment of advanced RCC. However, acquired drug resistance is a major hurdle in the clinical use of cabozantinib. Honokiol, a naturally occurring phenolic compound, has a great potential to downregulate c-Met-induced pathways. In this study, we found that a novel combination treatment with cabozantinib + Honokiol inhibits the growth of renal cancer cells in a synergistic manner through increased production of reactive oxygen species (ROS); and it significantly facilitates apoptosis-and autophagy-mediated cancer cell death. Activation of c-Met can induce Rubicon (a negative regulator of autophagy) and p62 (an autophagy adaptor protein), which can stabilize Nrf2. By utilizing OncoDB online database, we found a positive correlation among c-Met, Rubicon, p62 and Nrf2 in renal cancer. Interestingly, the combination treatment significantly downregulated Rubicon, p62 and Nrf2 in RCC cells. In a tumor xenograft model, this combination treatment markedly inhibited renal tumor growth *in* vivo; and it is associated with decreased expression of Rubicon, p62, HO-1 and vessel density in the tumor tissues. Together, cabozantinib + Honokiol combination can significantly inhibit c-Met-induced and Nrf2-mediated anti-oxidant pathway in renal cancer cells to promote increased oxidative stress and tumor cell death.

1. Introduction

Advanced renal cell carcinoma (RCC) still remains essentially incurable. Although there are significant advancements in treatment strategies, RCC remains a prevalent and challenging cancer type with increased incidence rate and poor survival outcomes in metastatic cases [1]. The heterogeneity of RCC renders it less susceptible to therapies, leading to the development of acquired therapeutic resistance and eventual treatment failure. Different combination treatments are being tested; however, after initial responses, most of the patients develop resistance. Thus, it is critical to explore the mechanistic pathways involved in therapeutic resistance.

The receptor tyrosine kinase (RTK), c-Met, is overexpressed and hyper active in both clear cell and papillary RCC [2,3]. Upon binding with the ligand hepatocyte growth factor (HGF), c-Met activates tumor-promoting pathways and can confer therapeutic resistance in RCC [4–6]. In our previous studies, we found that the induction of c-Met promotes activation of the redox-sensitive transcription factor Nrf2 and over-expression of the cytoprotective molecule heme oxygenase-1 (HO-1). Nrf2 regulates the expression of many phase II detoxifying

* Corresponding author. Division of Nephrology, Boston Children's Hospital, 300 Longwood Ave, Boston, MA 02115, USA.
E-mail address: soumitro.pal@childrens.harvard.edu (S. Pal).
[1] AS and SP are co-senior authors.

https://doi.org/10.1016/j.redox.2023.102945
Received 11 October 2023; Received in revised form 17 October 2023; Accepted 19 October 2023
Available online 21 October 2023

and antioxidant enzymes (like, HO-1) [7,8]. HO-1 is a stress-inducible enzyme and a member of the heat shock protein family [9]. HO-1 and its by-products classically function to maintain cellular homeostasis under stress [10]. However, Nrf2/HO-1 can also play a significant role in cancer growth and progression, primarily through the regulation of the redox state of cancer cells; it relieves the oxidative stress in cancer cells following therapeutic treatment [7]. Nrf2/HO-1 is over-expressed in cancer cells, including renal cancer, and its expression is further induced by radiation and chemotherapy [11,12]. p62 is an autophagy adaptor protein, which binds ubiquitylated protein aggregates and delivers them to the autophagosomes [13]. Interestingly, Sequestosome 1 (SQSTM1)/p62 can interact with Keap1 (Nrf2 substrate adaptor for the Cul3 E3 ubiquitin ligase); and this interaction allows p62 to sequester Keap1 into autophagosomes, which impairs the ubiquitination of Nrf2, leading to activation of the Nrf2 pathway and tumor cell survival [14,15].

Therapeutic agents promote cancer cell death through the induction of both apoptosis and autophagy. Although autophagy inhibition, combined with anticancer agents, could be therapeutically beneficial in some cases, autophagy induction by itself could lead to cell death in some apoptosis-resistant cancers [16]. Therapeutic agents can mediate tumor cell death through toxic autophagy that may facilitate apoptosis [17]; and the induction of canonical autophagy can sensitize the tumor cells to radiation therapy [18]. Reactive oxygen species (ROS) plays major role in drug-induced tumor cell death [19]. However, cancer cells can utilize the protective effects of Nrf2/HO-1 (through down-regulation and detoxification of ROS) as a shield from therapeutic agents [20,21]. We discovered that c-Met activation in RCC mediates growth-promoting signals against oxidative stress through Nrf2-HO-1 [7]. Thus, although Nrf2/HO-1 could be protective during early stages to overcome stress, it aggressively promotes tumor growth and cancer cell survival during therapeutic treatment.

RUBICON (a RUN domain-containing protein) is a component of the class III PI-3K complex and a novel Beclin-1-binding partner, which negatively regulates canonical autophagy and endocytosis [22]. It associates with UVRAG-Beclin-1 complex and suppresses autophagosome maturation and endocytic trafficking. The RUBICON protein is comprised of multiple functional domains that modulate intracellular signaling cascades [23]. It contains a RUN domain, which interacts with GTPases, two serine-rich regions (S–R), and a coiled-coiled domain (CCD), multiple helix-coil-rich repeats, and a cysteine-enriched FYVE--like domain [24]. RUBICON can be a potential target for autophagy-inducing therapeutics [25,26]. It is important to study if Rubicon plays any role in c-Met-Nrf2-induced cell survival pathway; and how this can be targeted.

Cabozantinib (XL-184) is a small molecule c-Met/RTK inhibitor and it has been approved for the treatment of advanced RCC [27]. However, as mentioned earlier, acquired drug resistance is a major hurdle in the clinical use of cabozantinib [28,29]. The anti-tumor effect of c-Met inhibitor(s) become significantly less as the tumors evolve to bypass the target molecule. To overcome these limitations, combination therapies show promise in other cancer subtypes. Combination therapy involves the administration of two or more therapeutic agents to achieve maximum therapeutic response while minimizing side effects.

Recently, natural compounds have gained significant attention due to their exceptional therapeutic effects in cancer [30–33]. Honokiol ($C_{18}H_{18}O_2$), a naturally occurring phenolic compound found in the bark, leaves, and seeds of Magnolia species (*Magnolia Obovata*), has gained interest for its potential health benefits. It possesses a wide range of pharmacological properties, including antioxidant, anti-inflammatory and anti-cancer effects [34,35]. We have demonstrated that Honokiol has a great potential to downregulate c-Met-induced and Ras-mediated pathway(s) in renal cancer cells [8]. It can also induce the cancer cells to be vulnerable to undergo apoptosis [36]. Thus, it will be interesting to explore the effect of a combination treatment with cabozantinib and Honokiol on c-Met-induced tumor-promoting pathway, and if it can significantly promote renal cancer cell death.

In the present study, we show that cabozantinib + Honokiol combination treatment promotes a synergistic effect to inhibit c-Met-induced renal cancer growth; and it induces oxidative stress-induced renal cancer cell death through increased apoptosis and autophagy. The combination treatment markedly downregulates Rubicon in RCC cells; this is associated with decreased expression of p62, and this can destabilize the anti-oxidant transcription factor, Nrf2. Together, cabozantinib + Honokiol combination can significantly inhibit c-Met-induced and Nrf2-mediated anti-oxidant pathway in renal cancer cells to promote increased oxidative stress and tumor cell death.

2. Materials and methods

2.1. Chemicals and reagents

Cabozantinib (XL-184) and Honokiol (HNK) were procured from Selleckchem (Houston, TX). The anti-Sqstm1/p62 (Cat. No. #88588), anti-Bcl-2 (Cat. No. #4223), anti-Bcl-xL (Cat. No. #2764), anti-Met (Cat. No. #3127), anti-LC3B (Cat. No. #2775) and anti-Nrf2 (Cat. No. #12721) antibodies were purchased from Cell Signaling Technology (Danvers, MA). It is important to note that most of the times, the anti-Nrf2 antibody gives a doublet band (as shown in the company catalog). Anti-β-actin (Cat. No. #A2228) was obtained from Sigma-Aldrich (Burlington, MA). Anti-Rubicon (Cat No. #Ab92388) and the CCK-8 kit were purchased from Abcam (Waltham, MA). Anti-Sp1 (Cat. No. #14027) was obtained from Santa Cruz Biotechnology (Dallas, TX), and anti-GAPDH (Cat. No. #A5028) was purchased from Selleckchem. For immunohistochemistry, anti-CD-31 (Cat. No. #550274) (1:50) was from BD Pharmingen (Woburn, MA); anti-Ki-67 (Cat. No. #14569880) and anti-Rubicon (Cat. No. #PA5-38017) (1:150) were from Invitrogen (Waltham, MA); anti-SQSTM1 (Cat. No. #88588) (1:100) was from Cell Signaling Technology; and anti-HO-1/HMOX1 (Cat. No. #10701-1-AP) (1:200) was from ProteinTech (Rosemont, IL). SQSTM1/p62 siRNA and transfection reagents were procured from Santa Cruz biotechnology.

2.2. Cell lines

Human renal cancer cell lines (786-0, ACHN, Caki-1 and Caki-2) were obtained from the American Type Culture Collection (ATCC, Rockville, MD) in 2015. All human cell lines were reauthenticated through short tandem repeat profiling by ATCC. 786-0, ACHN, Caki-1, and Caki-2 cell lines were maintained in RPMI 1640 medium. The culture media were supplemented with 10% heat-inactivated fetal bovine serum and 1% penicillin/streptomycin antibiotics (Invitrogen, Carlsbad, CA). Normal renal proximal tubular epithelial cells (RPTEC) were purchased from Lonza and cultured in renal epithelial cell basal medium with SingleQuots growth supplements (Lonza, Portsmouth, NH).

2.3. Generation of CRISPR/Cas9-mediated knockout cells

Renal cancer cells (786-0) were co-transduced with lentiviral particles encoding Cas9 and gRNA targeting either RUBCN (Rubicon) or control (Thermo Fisher, Waltham, MA). The stable transduced clones were selected through antibiotic containing media, and confirmed through Western blot analysis to check the expression of Rubicon. The clones exhibiting verified Rubicon knockout (KO) were chosen for experiments.

2.4. Cell viability

786-0 and ACHN cells were seeded in 96-well plates at a density of $1x10^4$ cells/well and incubated overnight. Next day, media was replaced with the serum-deficient media and incubated for 24 h. After serum starvation, the cells were treated with XL-184 (1–30 μM), HNK (5–50 μM) or vehicle for 24 h. Following treatments, the CCK-8 kit was used to

measure viability according to the manufacturer's protocol. For the combination treatment experiments, cells were seeded similarly in 96-well plates, and treated with combinations of XL-184 (1, 2, and 5 μM), HNK (5, 10, and 20 μM) or vehicle for 24 h, followed by the CCK-8 assay. For further studies, 5 μM of XL-184 and 20 μM of HNK were used.

2.5. Assessment of total ROS levels

Cells were seeded with a seeding density of 1×10^5 cells/well in 6-well plates and allowed to adhere overnight. Cells were serum starved for 12 h to synchronize the cell growth. Cells were then treated with combinations of XL-184 (5 μM), HNK (20 μM) or vehicle for 6 h. Cells were then trypsinized and stained using ROS-ID total ROS detection kit from Enzo Life Sciences (Plymouth, MA), according to the manufacturer's protocol. Subsequently, flow cytometry was performed using a BD FACSCelesta cell analyzer.

2.6. Autophagy assay

Briefly, $1x10^5$ cells were seeded in 6-well tissue culture plates. Next day, Cells were then treated with combinations of XL-184 (5 μM), HNK (20 μM) or vehicle for 24 h. Following treatment, cells were trypsinized, washed with 1X PBS and stained using CYTO-ID® Autophagy detection kit from Enzo Life Sciences (Plymouth, MA), according to the manufacturer's protocol. Autophagy was then assessed using BD FACSCelesta cell analyzer.

2.7. Apoptosis assay

Cells were seeded and treated similarly as for the autophagy assay. Following treatments, the cells were trypsinized, washed with 1X PBS and stained with an Annexin V-APC and propidium iodide using Apoptosis detection kit from ThermoFisher Scientific (Waltham, MA) as previously described [37]. The cells were then analyzed by flow cytometry using a BD FACSCelesta cell analyzer.

2.8. Nuclear and cytosolic fractionation

Cells were treated as mentioned for autophagy assay. Following treatment, cells were lysed and nuclear/cytoplasmic fractions were separated using NE-PER Nuclear and Cytoplasmic Extraction Reagents Kit (Thermo Fisher Scientific, Waltham, MA) according to the manufacturer's protocol.

2.9. Western blot

Cells were seeded and treated with combinations of XL-184, HNK or vehicle as mentioned before. Following treatments, the cells were harvested and cell lysates were prepared. Protein samples were resolved on sodium dodecyl sulfate–polyacrylamide (SDS-PAGE) gel and transferred to the polyvinylidene difluoride membranes (Milipore Corporation, Burlington, MA). The membranes were blocked in a 5% milk, incubated with specific primary antibodies over night at 4 °C, and then followed by incubation with an appropriate HRP-linked secondary antibody. The membranes were processed for enhanced chemiluminescence detection (Thermo Fisher Scientific) using the ChemiDoc Imaging System (Bio-Rad, CA).

2.10. siRNA transfection

786-0 and ACHN cells were seeded in 6-well plate at 1×10^5 cells/well and incubated overnight in an antibiotic free media. Transfection was performed according to the manufacturer's protocol and the gene knockdown was confirmed by Western blot.

2.11. Tumor xenograft model

To investigate tumor growth, 786-0 cells were subcutaneously injected into dorsal flank of 8-week-old male athymic nude mice and observed for the formation of tumors. The mice were then divided into four treatment groups ($n = 5$ mice per group): vehicle, XL-184, HNK, and XL-184 + HNK. Once the palpable tumor growth was observed, mice were treated with XL-184 (15 mg/kg), HNK (2 mg/kg) and XL-14 + HNK every alternate day for three weeks via intraperitoneal injection (IP). Tumor volumes were measured using a digital caliper, and the tumor volumes were calculated using the standard method $V = 1/2(h \times w \times w)$ [38]. The excised tumors were promptly snap-frozen in OCT (Sakura Finetek, Torrance, CA) and stored at −80 °C until further use. All animal experiments were conducted with approval from the animal care and use committee at Boston Children's Hospital (BCH) and in accordance with the National Institutes of Health (NIH) guidelines for the care and use of laboratory animals.

2.12. Immunohistochemistry

The tissue sections were prepared from frozen tumors and fixed with pre-chilled acetone for 10 min. Following fixation, sections were blocked using 10% BSA and then incubated with primary antibodies overnight at 4 °C. Afterwards, the sections were incubated with species-specific horseradish peroxidase-conjugated secondary antibodies (Abcam, Waltham, MA). The sections were thoroughly washed twice with 1X PBS between each step. For substrate visualization, sections were incubated with DAB (3,3′-Diaminobenzidine, Vector laboratories, Newark, CA). The sections were counterstained with Mayer's Hematoxylin (G-Biosciences, St. Louis, MO). Photomicrographs were captured using the Nikon Eclipse photomicroscope at 400X magnification. DAB intensity was quantified using ImageJ software (v. 1.54f), and bar graphs were plotted to show the mean intensity of DAB.

2.13. Statistical analysis

Statistical analysis was performed using GraphPad Prism (version 9.0). For *in vitro* studies, we conducted either Student's t-test for two groups or one-way ANOVA for three or more groups. SynergyFinder 3.0 tool was used to find synergy with Highest single agent (HSA) reference model [39,40]. For *in vivo* studies, data were analyzed using two-way ANOVA followed by Tukey's multiple comparison test. For immunohistochemistry, groups were analyzed using one way ANOVA followed by Holm-Sidak multiple comparison test. Differences with p-values <0.05 was considered statistically significant.

3. Results

3.1. A combination treatment with cabozantinib (XL-184) and Honokiol (HNK) inhibits the growth of renal cancer cells in a synergistic manner

As mentioned before, the receptor tyrosine kinase (RTK), c-Met, is highly expressed in renal cancer cells (both clear cell and papillary types) and promotes tumor growth [41–43]. The expression levels of c-Met mRNA in tumor samples and paired normal tissues were analyzed using GEPIA database [44]. The analysis showed that c-Met was markedly higher in renal cancer subtypes compared to normal tissues (Fig-1A). Additionally, the interactive bodymap (Fig-1B) showed the median mRNA expression of c-Met in tumor (red) and normal (green) tissues [44]. As shown in Fig-1C and 1D, analyses through UALCAN online tool clearly indicate that c-Met expression was significantly upregulated in both clear cell and papillary renal cell carcinoma; and it was increased at different clinical stages compared with normal tissues [45,46]. We also confirmed that compared with normal renal epithelial cells (RPTEC), c-Met was markedly upregulated in different human renal cancer cell lines (786-0, ACHN, Caki-1 and Caki-2) (Fig-1E).

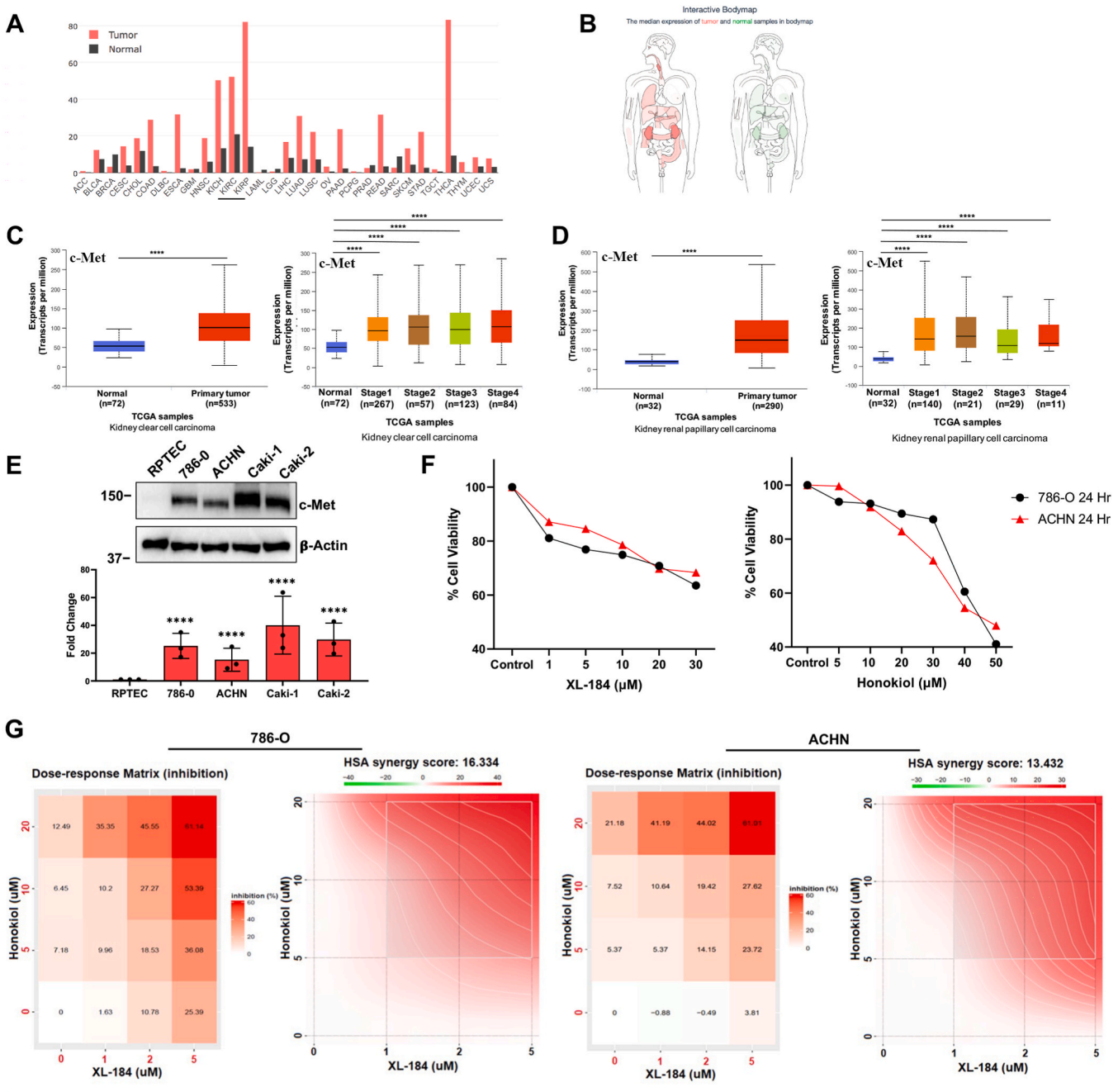

Fig. 1. c-Met is overexpressed in RCC and a combination of XL-184 and Honokiol (HNK) synergistically restricts renal cancer cell growth. (A) The gene expression profile of c-Met in patient tumor samples and paired normal tissues in different cancer types was evaluated using GEPIA database. c-Met is overexpressed (underlined) in clear cell (KIRC) and papillary (KIRP) type RCC. **(B)** The body map representing differential median expression of c-Met in normal and various cancer types was analyzed using GEPIA database. **(C–D)** Gene expression of c-Met in normal and primary tumor samples in (C) human clear cell renal carcinoma (ccRCC), and (D) papillary RCC were analyzed by UALCAN database (*left panels*). c-Met expression in different stages of (C) ccRCC and (D) papillary RCC were analyzed in a similar way (*right panels*). ****$p < 0.0001$. **(E)** Expression of c-Met in normal RPTEC versus RCC cells (786-0, ACHN, Caki-1 and Caki-2) were analyzed by Western blot. Molecular weight markers (kDa) are on the left. The bar graphs under the Western blots represent the relative expression of c-Met by densitometry, where the signals were normalized to the expression of an internal control, β-Actin. The columns represent the average ± SD of relative intensities ($n = 3$). Representative of three. ****$p < 0.0001$ compared with RPTEC. **(F)** 786-0 and ACHN renal cancer cells were treated with increasing concentrations of XL-184 (1–30 μM), HNK (5–50 μM) or vehicle for 24 h. Control was treated with vehicle alone. Following treatments, cell viability was assessed using CCK-8 assay; the graphs represent percent cell viability of 786-0 (*black*) and ACHN (*red*) cells. Representative of three experiments. **(G)** 786-0 and ACHN cells were treated with combinations of XL-184 (1–5 μM), HNK (5–20 μM) or vehicle alone for 24 h. Following treatments, cell viability was evaluated by CCK-8 assay. Heat maps represent the percent growth inhibition of 786-0 and ACHN cells (*left panels*) following either individual or combination treatment. Synergy plots (*right panels*) represent synergism among XL-184 and HNK treatments. Representative of three different experiments. Positive score (red) indicates the synergism, whereas negative score (green) indicates antagonistic effect. (For interpretation of the references to colour in this figure legend, the reader is referred to the Web version of this article.)

Cabozantinib (XL-184), is a small molecule inhibitor of c-Met/RTKs and an approved agent for the treatment of renal cancer [47]. However, most of the patients inevitably develop therapeutic resistance and the tumor progresses [28]. Honokiol has anti-tumorigenic properties [48]; and we have demonstrated that it can inhibit c-Met-induced pathways [36]. We first analyzed the viability of two renal cell carcinoma (RCC) cell lines, 786-0 (clear cell type) and ACHN (papillary type) following cabozantinib and Honokiol treatment; and we observed that there was a dose-dependent decrease in cell viability with both cabozantinib and Honokiol (Fig-1F). Next, we tested the effect of a combination treatment using cabozantinib and Honokiol on the growth of 786-0 and ACHN cells. We treated the cells with a combination of cabozantinib (1–5 uM) and Honokiol (5–20 uM), and the cell viability was assessed. We found that the combination of cabozantinib + Honokiol significantly inhibited cell viability (~61%) in both the cell lines, compared with their individual doses (Fig-1G). We then evaluated the synergistic effect of these two agents on cell viability using SynergyFinder 3.0 tool [49] and we obtained a strong synergy between cabozantinib and Honokiol in both the cell lines (Fig-1G). This data clearly suggest that Honokiol can potentiate the anti-cancer efficacy of cabozantinib; and it can also help to overcome the limitation of cabozantinib treatment alone in renal cancer.

3.2. *Cabozantinib (XL-184) and Honokiol combination elevates the level of intracellular reactive oxygen species (ROS) and induces cancer cell death through increased autophagy and apoptosis*

Elevated ROS levels following therapeutic treatments play a crucial

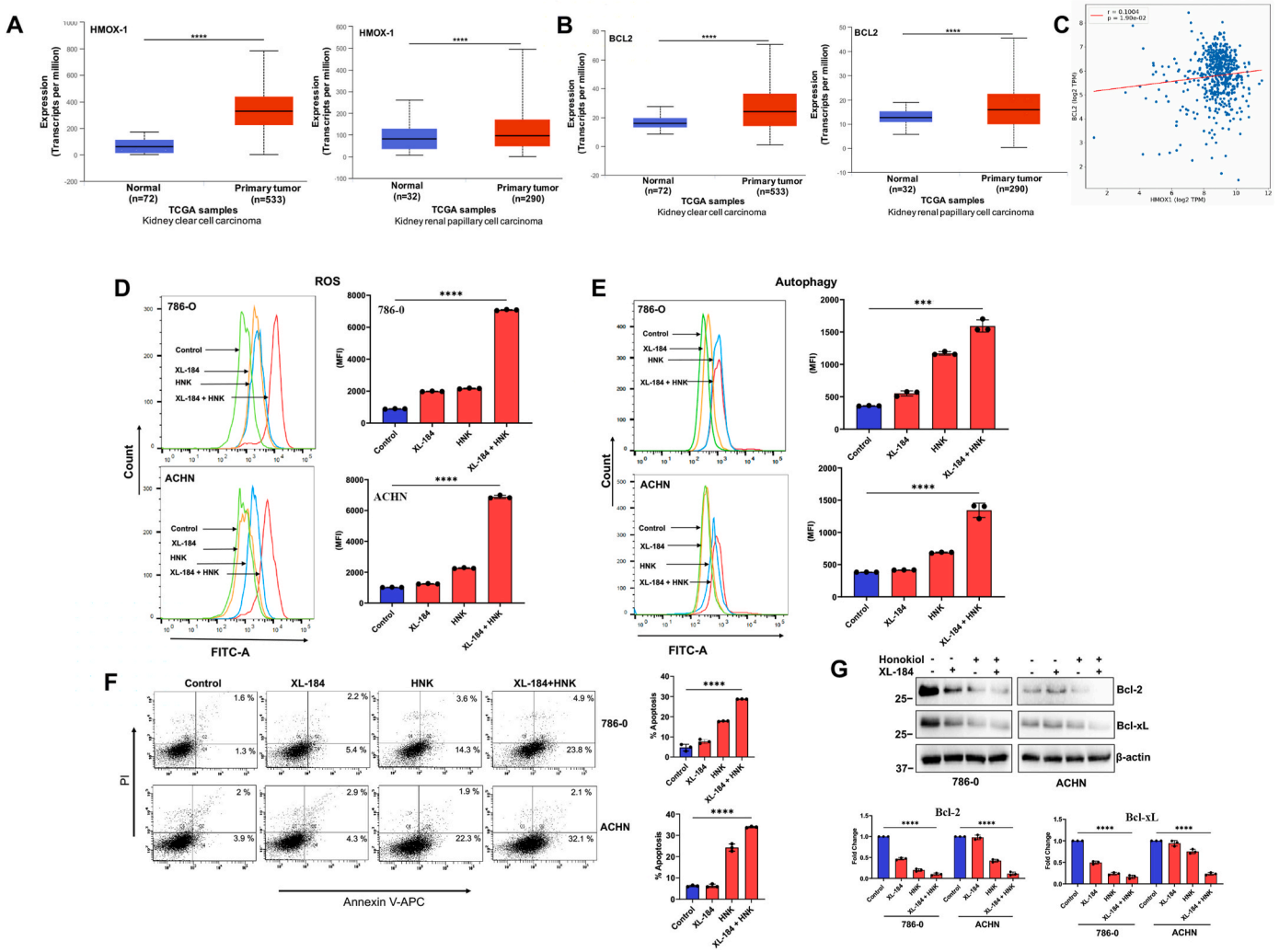

Fig. 2. Combination of XL-184 and Honokiol (HNK) significantly induces ROS generation, and mediates autophagy and apoptosis in renal cancer cells. **(A-B)** Gene expression of (A) HMOX-1(HO-1) and (B) BCL2 in normal and primary tumor samples in human kidney clear cell carcinoma (ccRCC) (*left*) and papillary cell carcinoma (*right*) were analyzed using UALCAN database (****p < 0.0001). **(C)** Correlation analysis between HMOX-1 and BCL2 mRNA expression in human ccRCC was performed using OncoDB database. **(D)** 786-0 and ACHN cells were treated with combinations of XL-184 (5 μM) and HNK (20 μM) for 6 h. The control group was treated with vehicle alone. Following treatments, cells were stained with ROS-ID dye and total ROS generation was measured by flow cytometry and quantifications are presented as bar graphs (*right panel*). Data represent the mean ± SD of triplicate readings; representative of three different experiments. **(E)** 786-0 and ACHN cells were treated similarly as described in (D) for 12 h. Following treatment, cells were stained with Cyto-ID dye and autophagy was determined by flow cytometry and quantifications are presented as bar graphs (*right panel*). Data represent the mean ± SD of triplicate readings; representative of three different experiments. **(F)** 786-0 and ACHN cells were treated similarly as described in (D) for 24 h. Following treatments, cells were stained with Annexin V (APC) and propidium iodide (PI), and the apoptotic indices were analyzed by flow cytometry and the percentage of total (early + late) apoptotic cells were quantified and represented as bar graphs (right panel). Data represent the mean ± SD of triplicate readings; representative of three different experiments. **(G)** 786-0 and ACHN cells were treated similarly as described in (F), followed by Western blot analysis of Bcl-2 and Bcl-xL. Molecular weight markers (kDa) are on the left. The bar graphs under the Western blots represent the relative expression of Bcl-2 and Bcl-xL by densitometry, where the signals were normalized to the expression of an internal control, β-Actin. The columns represent the average +/- SD of relative intensities (n = 3). Representative of three. In D-G, ***p < 0.001 and ****p < 0.0001 compared with the control.

role in mediating tumor cell death (both apoptosis and autophagy) through increased oxidative stress [50,51]. As mentioned earlier, the anti-oxidant HO-1/HMOX-1, play a vital role in relieving oxidative stress and promoting cancer cell survival [52]. Using UALCAN database, we analyzed the expression of HMOX-1 and anti-apoptotic BCL2 in primary renal tumors (both clear cell and papillary types) compared with normal tissues [45,46]. We found that both HMOX-1 and BCl2 were significantly higher in primary tumors (Fig-2A and 2B). To understand the correlation between HMOX-1 and BCL2, we utilized OncoDB online database [53]. It showed that both the genes were positively correlated in RCC (Fig-2C). Thus, it is very important to overcome the effect of these anti-oxidant regulatory mechanism(s) and sustain the oxidative stress to induce cancer cell death following therapeutic treatments.

We evaluated the total cellular ROS in renal cancer cells following treatments with combinations of cabozantinib and Honokiol. We found ~2-fold increase in total cellular ROS level following individual treatment with either cabozantinib or Honokiol compared with controls. However, cabozantinib + Honokiol combination treatment significantly increased the total ROS (~7-fold) compared with controls (Fig-2D).

Therapeutic agents can induce autophagy, particularly, toxic autophagy, to promote cancer cell death [54]. We found that cabozantinib + Honokiol combination treatment markedly increased cellular autophagy in both 786-0 and ACHN cells compared with controls and individual treatments (Fig-2E). We also evaluated the total apoptotic cells (early + late) following combination treatment; and we found that cabozantinib + Honokiol combination significantly induced cellular apoptosis (early + late) in both 786-0 and ACHN cells compared with controls (Fig-2F). In addition, we also confirmed the expression of apoptosis markers, Bcl-2 and Bcl-xL (anti-apoptotic), which were markedly decreased after the combination treatment (Fig-2G). Together, our data clearly suggest that cabozantinib + Honokiol combination therapy significantly induce the oxidative stress in RCC cells to promote cell death through increased autophagy and apoptosis.

3.3. Cabozantinib and Honokiol combination treatment downregulates novel effector molecules (Rubicon, p62 and Nrf2) of the c-met pathway

We have previously reported that the c-Met pathway plays a crucial role in therapeutic resistance against oxidative stress through the regulation of Nrf2; and it can inhibit renal cancer cell death through the downregulation of apoptosis and autophagy [7]. As mentioned before, Rubicon is a negative regulator of autophagy; and p62 is an important molecule for the stabilization of Nrf2 during oxidative stress. Analyses through UALCAN online tool [45,46] clearly indicated that both Rubicon and p62 (SQSTM1) expression were markedly upregulated in renal cell carcinoma (both clear cell and papillary types) (Fig-3A and 3B). To understand the correlation among c-Met, Rubicon, p62 and Nrf2, we utilized OncoDB online database [53]. It showed that there are positive correlations between c-Met-Rubicon, c-Met-p62, c-Met-Nrf2, Rubicon-Nrf2, Rubicon-p62 and Nrf2-p62 in RCC (Fig-3C).

We checked how the cabozantinib + Honokiol combination treatment can alter the expression of Rubicon and p62. We found that Rubicon, p62 and Nrf2 are highly overexpressed in RCC cells (both 786-0 and ACHN) compared with normal renal epithelial cells (Fig-3D); and the activation of c-Met following HGF treatment further induced the expression of these molecules (Fig-3E). Interestingly, cabozantinib + Honokiol combination treatment significantly inhibited the expression of Rubicon, p62 and Nrf2 in both 786-0 and ACHN cells (Fig-3F). We also confirmed that the combination treatment lead to a decreased nuclear localization of Nrf2 (Fig-3G). As mentioned before, SQSTM1/p62 plays a crucial role in the nuclear translocation of Nrf2 through destabilization of the Keap1-Nrf2 complex. Thus, we sought to determine the impact of p62 knockdown on the level of Nrf2 in RCC cells. We found that the knockdown of p62 resulted in a low basal level of Nrf2; and the combination treatment with cabozantinib + Honokiol further decreased the Nrf2 level (Fig-3H). Together, our observations suggest that cabozantinib + Honokiol combination treatment can downregulate Rubicon that may lead to increased autophagy-mediated cancer cell death. The combination treatment also downregulates the level of Nrf2, possibly through the inhibition of p62; and this may result in increased oxidative stress to promote renal cancer cell death.

3.4. Deletion of Rubicon facilitates the induction of ROS level and increases apoptotic cell death following cabozantinib and Honokiol combination treatment in renal cancer cells

Although cabozantinib + Honokiol combination treatment could downregulate Rubicon, we wanted to check if the complete knockout of Rubicon can further increase the efficacy of the therapeutic combination in renal cancer cells. We utilized stable RCC cells, where RUBICON has been knocked out (KO) through CRISPR-Cas-9 (along with control). We observed that the combination treatment further increased the ROS level in Rubicon-KO cells compared with control clones (Fig-4A). We also evaluated the status of apoptosis in these cells. We found that compared to control clones, cabozantinib + Honokiol combination treatment further increased the total apoptotic cells in Rubicon-KO clones of renal cancer cells (Fig-4B). We also confirmed the status of markers for apoptosis (Bcl2 and Bcl-xL) and autophagy (LC3B), which were further downregulated in Rubicon-KO cells following combination treatment (Fig-4C, *left panel*). Finally, we evaluated the expression of p62 and Nrf2; and we found that both p62 and Nrf2 were further downregulated in Rubicon-KO cells following cabozantinib + Honokiol combination treatment (Fig-4C, *right panel*). Together, these observations suggest that cabozantinib + Honokiol combination treatment promotes oxidative stress-induced renal cancer cell death through the downregulation of Rubicon, which can be associated with decreased p62 and Nrf2. The complete knockout of Rubicon further facilitates the cell death pathway for this combination treatment; and these observations are supportive to our findings. However, in addition to the downregulation of Rubicon, it is possible that this combination treatment can also partly inhibit some other tumor-promoting pathway(s).

3.5. Cabozantinib and Honokiol combination treatment inhibits renal tumor growth in vivo; and it is associated with decreased Rubicon, p62, HO-1 and vessel density in the tumor tissues

Our *in vitro* studies clearly suggest that cabozantinib + Honokiol combination treatment can mediate a synergistic effect to promote oxidative stress-induced renal cancer cell death through the downregulation of Rubicon and p62; and this can destabilize the anti-oxidant transcription factor, Nrf2. To evaluate the physiological significance of our *in vitro* findings, we tested the effect of this combination treatment in a renal tumor xenograft model. By utilizing the established doses of cabozantinib and Honokiol [7,26], the combination treatment significantly decreased the tumor volumes compared with either vehicle-treated controls or the individual treatment groups (Fig-5A and 5B). We then checked the expression of molecular markers in tumor tissues of the treatment groups. As shown in Fig-6, the tumor vessel density (CD31) and proliferation index (Ki-67) was markedly reduced in the tumors following combination treatment. We then evaluated the expression of Rubicon, p62 and HO-1 (a functional effector of Nrf2). Interestingly, cabozantinib + Honokiol combination treatment markedly downregulated Rubicon, p62 and HO-1 in renal tumor tissues. Together, our *in vitro* as well as *in vivo* findings clearly suggest the cabozantinib + Honokiol combination treatment can be a potential therapeutic strategy to promote renal cancer cell death through the inhibition of Nrf2 and increased oxidative stress.

4. Discussion

New therapeutic combinations are essential for the treatment of advanced renal cell carcinoma (RCC) and to overcome therapeutic

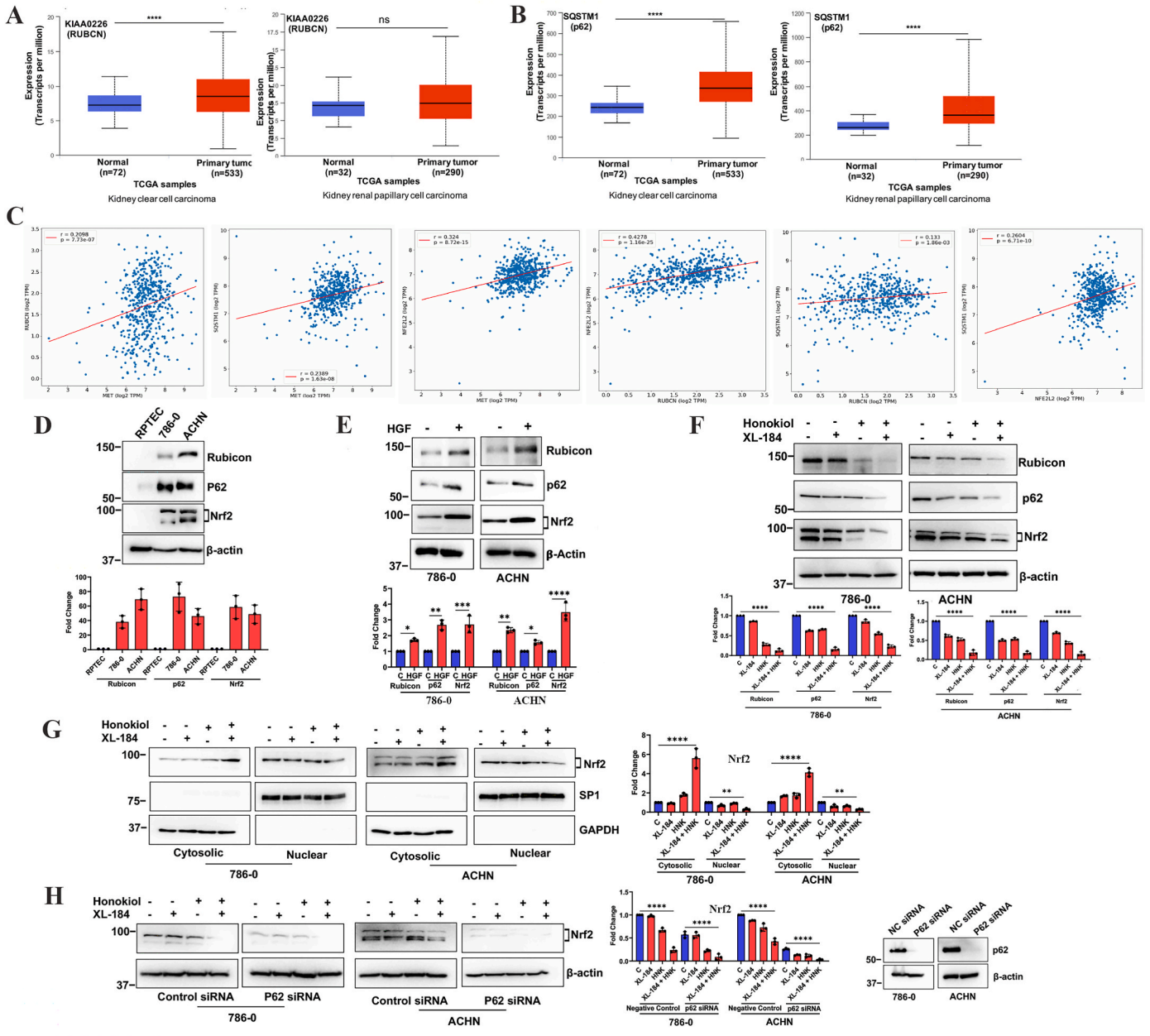

Fig. 3. Combination of XL-184 and Honokiol (HNK) effectively restricts c-Met induced upregulation of Rubicon, p62 and Nrf2 in renal cancer cells. (**A-B**) Gene expression of (A) KIAA0226 (RUBCN/Rubicon) and (B) SQSTM1 (p62) in normal and primary tumor samples in human kidney clear cell carcinoma (ccRCC) (*left*) and papillary cell carcinoma (*right*) was analyzed by UALCAN (****p < 0.0001; ns = non-significant). **(C)** Correlation analysis between c-Met-RUBCN (Rubicon), c-Met-SQSTM1 (p62), c-Met-NFE2L2 (Nrf2), RUBCN-NFE2L2, RUBCN-SQSTM1 and NFE2L2-SQSTM1 mRNA expression in human ccRCC was performed by OncoDB. **(D)** Basal protein expression of Rubicon, p62 and Nrf2 in normal renal epithelial cells (RPTEC) and renal cancer cells (786-0 and ACHN) were analyzed by Western blot. **(E)** Serum starved 786-0 and ACHN cells were treated with HGF (50 ng/mL)/vehicle for 24 h and the expression of Rubicon, p62 and Nrf2 were analyzed by Western blot. **(F)** 786-0 and ACHN cells were treated with combinations of XL-184 (5 μM), HNK (20 μM) or vehicle alone for 24 h; following treatments, lysates were collected and Western blot was performed to study the expression of Rubicon, p62 and Nrf2. **(G)** 786-0 and ACHN cells were treated as mentioned in (F) and cytosolic and nuclear fraction were prepared and Western blot was performed for Nrf2. Sp1 and GAPDH were used as loading controls for nuclear and cytosolic fractions, respectively. **(H)** 786-0 and ACHN cells were transfected with either control siRNA/p62 siRNA; cells were then treated with combinations of XL-184 (5 μM), HNK (20 μM) or vehicle for 24 h. Following treatments, lysates were collected and Western blot was performed for Nrf2. The knockdown of p62 following siRNA transfection was confirmed by Western blot (*right panel*). In D-H, Molecular weight markers (kDa) are shown on the left. The bar graphs under/beside the Western blots represent the relative expression of respective proteins by densitometry, where the signals were normalized to the expression of an internal control, β-Actin/GAPDH/Sp1. The columns represent the average +/- SD of relative intensities (n = 3). Representative of three different experiments. *p < 0.05, **p < 0.01, ***p < 0.001 and ****p < 0.0001.

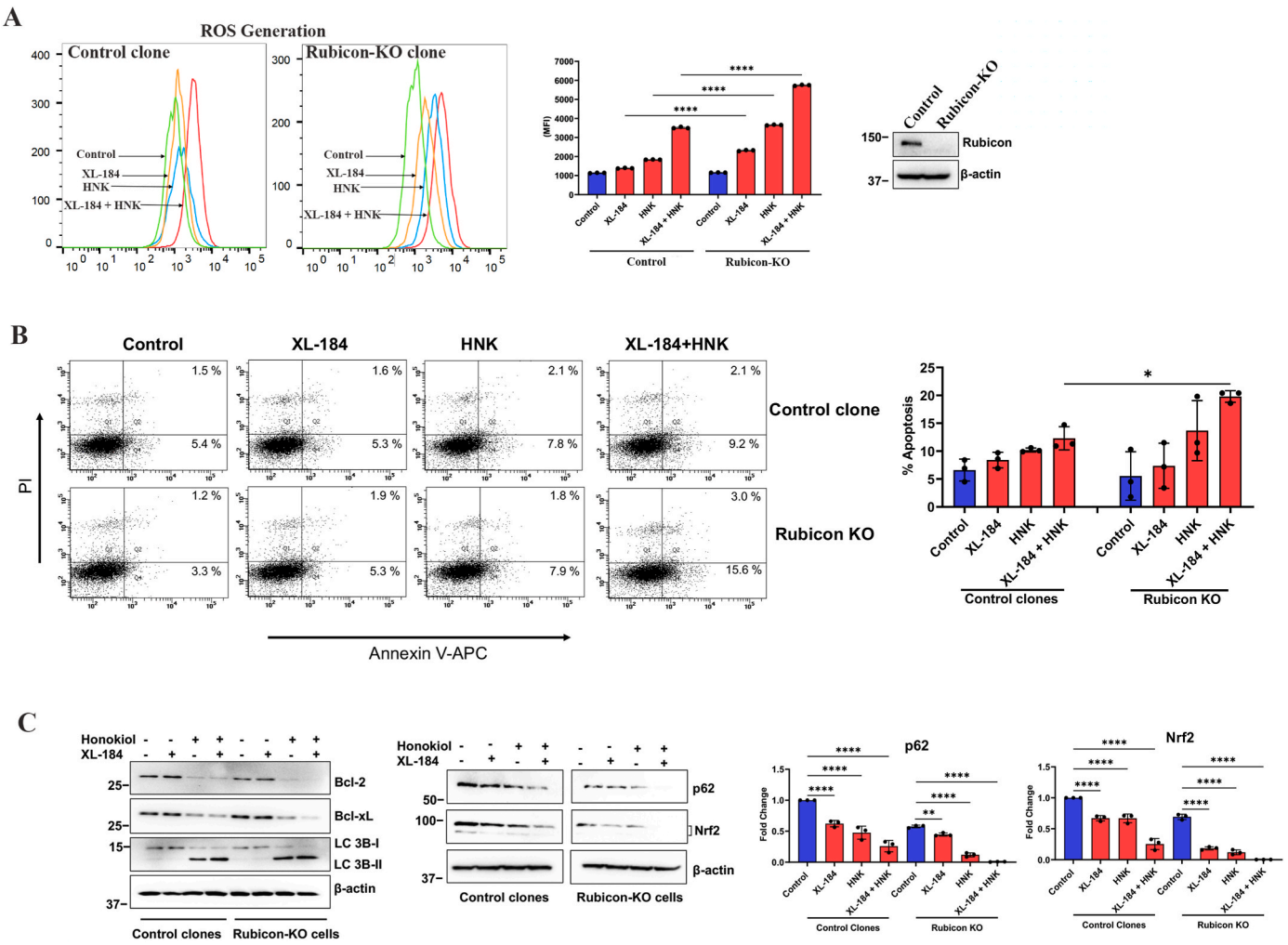

Fig. 4. Rubicon Knockout (KO) enhances XL-184- and HNK-mediated ROS generation and apoptosis in RCC cells. (A) Control and Rubicon KO CRISPR clones were treated with combinations of XL-184 (5 μM), HNK (15 μM) or vehicle for 6 h. Following treatments, cells were stained with ROS-ID dye and total ROS generation was measured by flow cytometry and quantifications are presented as bar graphs (*right panel*). Data represent the mean ± SD of triplicate readings; representative of three different experiments. The knockout of Rubicon was confirmed by Western blot (*right panel* beside the bar graph). **(B)** Control clones and Rubicon KO clones were treated similarly as described in (B) for 24 h. Cells were then stained with Annexin V (APC) and propidium iodide (PI), and apoptotic indices were analyzed by flow cytometry and the percentage of total (early + late) apoptotic cells were quantified and represented as bar graphs (right panel). Data represent the mean ± SD of triplicate readings; representative of three different experiments. **(C)** Control clones and Rubicon KO clones were treated similarly as described in (B) for 24 h. Lysates were collected and Western blot was performed for Bcl-2, Bcl-xL, LC 3b I/II, p62, Nrf2 and β-actin. Molecular weight markers (kDa) are on the left. The bar graphs beside the Western blots represent the relative expression of p62 and Nrf2 by densitometry, where the signals were normalized to the expression of an internal control, β-Actin. The columns represent the average +/- SD of relative intensities (n = 3). Representative of three different experiments. In A- C, *p < 0.05, **p < 0.01, and ****p < 0.0001.

resistance. c-Met is highly overexpressed in renal cancer and promotes tumor growth; and it can induce therapeutic resistance [3,6,55]. Cabozantinib is a c-Met/RTK inhibitor, which is currently being used for the treatment of RCC patients. By targeting RTK-induced signaling pathways, cabozantinib hinders tumor angiogenesis, proliferation, and metastasis. However, in advanced RCC, patients inevitably develop resistance against cabozantinib [28]. As mentioned before, Honokiol is a naturally occurring phenolic compound, which can inhibit c-Met-induced tumor-promoting pathways [8]. In this study, we have shown how a novel combination treatment using cabozantinib and Honokiol can restrict the growth of renal cancer cells; and how it can induce tumor cell death through increased oxidative stress by the inhibition of anti-oxidant transcription factor, Nrf2.

Most of the therapeutic agents induce increased oxidative stresses within cancer cells through the generation of ROS, and they promote cell death pathways through apoptosis and autophagy [56]. Depending on the context, the process autophagy can play a dual role in terms of cancer progression versus inhibition. Although the inhibition of autophagy can be beneficial to treat certain cancer types/stages, lot of therapeutic agents promote cancer cell death through induced autophagy, often termed as toxic autophagy [57,58]. Also, autophagy can play a crucial role in mediating cancer cell death in apoptosis-resistant cells [59]. In this study, we found that cabozantinib + Honokiol can promote a synergistic effect in mediating renal cancer cell death through increased reactive oxygen species (ROS) generation, and thereby facilitating cellular apoptosis and autophagy.

The c-Met pathway can downregulate both apoptosis and autophagy in renal cancer cells [8,60]. As discussed earlier, Rubicon is a negative regulator of autophagy [61,62]; and according to the available database (as shown in Fig-3C), there is a positive correlation between c-Met and Rubicon in renal cancer. In this study, we found that the activation of c-Met markedly induces Rubicon in RCC cells, both clear cell and papillary types. p62 (SQSTM1) is an autophagy adaptor protein [13]; and the inhibition of autophagy can lead to increased accumulation of

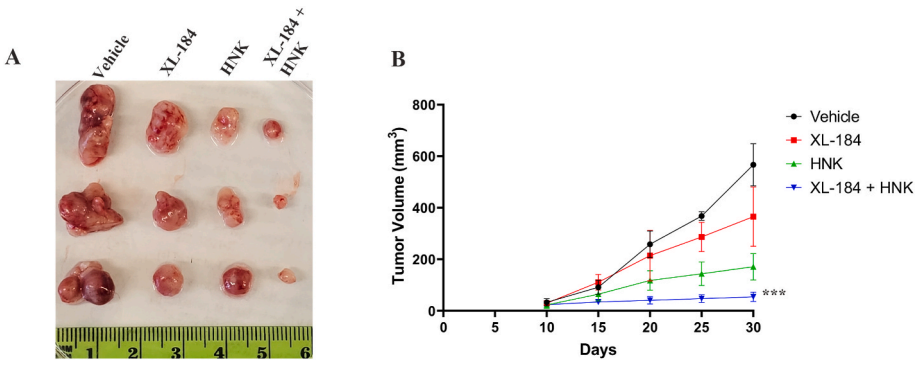

Fig. 5. XL-184 and HNK combination treatment markedly restricted renal tumor growth in a xenograft model. 786-0 cells were subcutaneously injected into flanks of athymic nude mice. Once palpable tumors were formed, mice were injected (IP) with combinations of XL-184 (15 mg/kg), HNK (2 mg/kg) or vehicle alone ($n = 5$ per group) for 3 weeks, and tumor volumes were measured. **(A)** Representative photographs of tumors excised on 30th day following tumor injection. **(B)** Line graph showing tumor volumes recorded at indicated time points. ***p < 0.001 compared with vehicle-treated control.

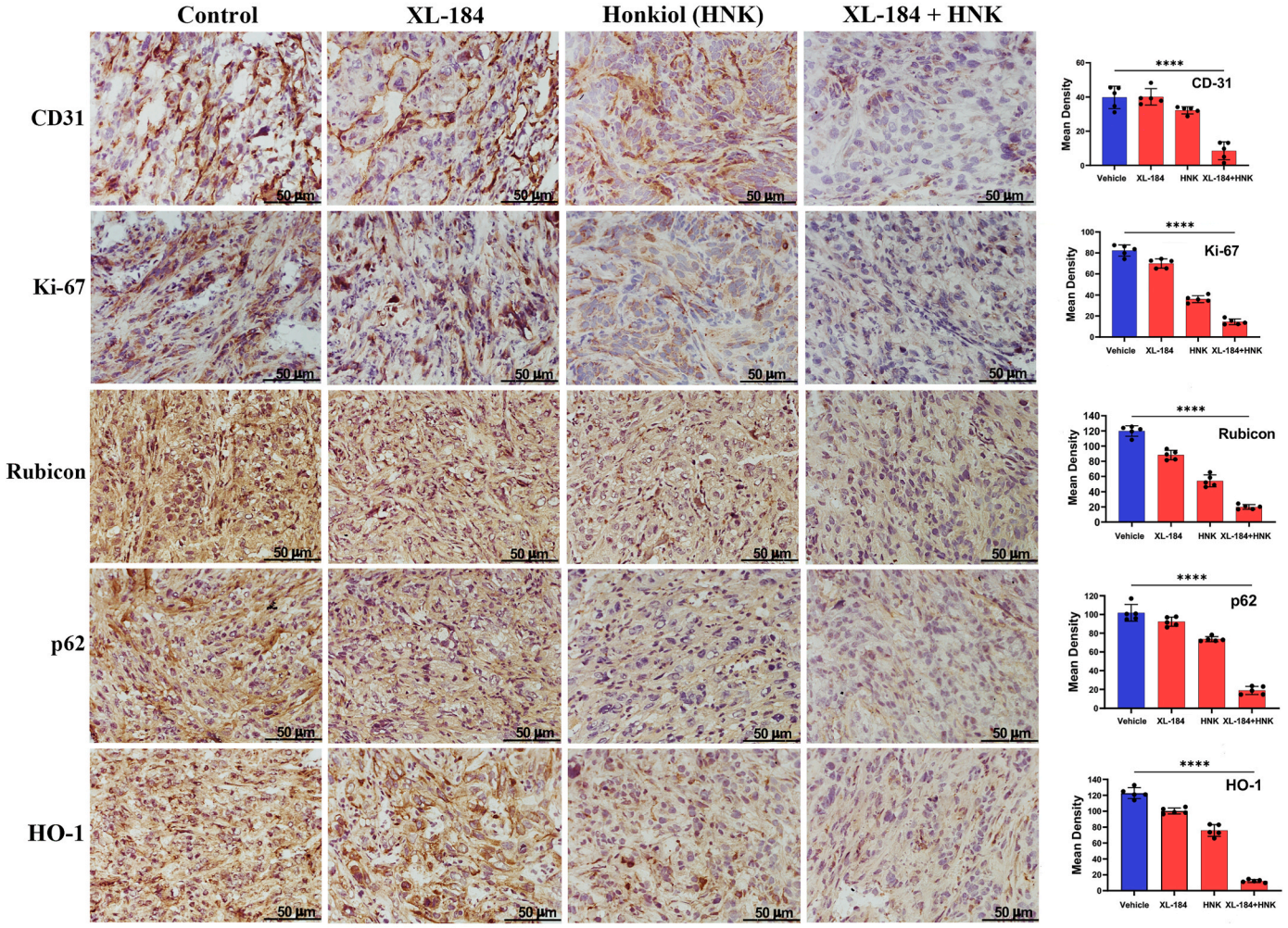

Fig. 6. Combination treatment of XL-184 and HNK significantly decreased the expression of CD31, Ki-67, Rubicon, p62, and HO-1 in renal tumor tissues. Renal tumors sections obtained from athymic nude mice post XL-184 and HNK treatments were processed for immunohistochemistry. The figure illustrates representative photomicrographs (magnification ×400) showing immunohistochemical expression of CD31, Ki-67, Rubicon, p62 and HO-1 in harvested tumor tissues. Magnification: ×400. Columns, average values of intensity of stained proteins; bars, ±SD of five different readings. ****p < 0.0001 compared with vehicle-treated control.

p62. According to the available database (as shown in Fig-3C), there is a positive correlation between Rubicon and p62 in renal cancer cells. p62 can play a critical role in the stabilization of Nrf2 through the degradation of Keap-1 [14,63]. Nrf2 is then translocated to the nucleus, where it promotes the transcription of anti-oxidant molecules, like, HO-1. Nrf2-HO-1 pathway is important for normal physiological processes and cytoprotection during oxidative stress [10,64]. However, cancer cells hijack this pathway for their own survival [7,65]. The over-activation of Nrf2 has been observed in various cancer types and has been associated with unfavorable treatment outcomes and therapeutic resistance [66]. We have reported that the activation of c-Met can induce Nrf2-HO-1 in renal cancer cells [7]. Importantly, p62 itself can also be regulated by Nrf2, establishing a positive feedback loop. Nrf2 activation enhances p62 expression, which in turn amplifies Nrf2 stabilization and activity [67]. Perturbation of the Nrf2-p62 axis can disrupt antioxidant responses and increase the vulnerability to oxidative damage. Interestingly, in this study, we found that cabozantinib + Honokiol combination treatment can markedly downregulate Rubicon, p62 and Nrf2 in RCC cell. Also, it significantly prevents the nuclear translocation of Nrf2. Thus, our findings suggest that that Honokiol can significantly facilitate cabozantinib-mediated renal cancer cell death through the inhibition of Rubicon-p62, destabilization of Nrf2 and increased oxidative stress.

Although cabozantinib + Honokiol combination treatment could downregulate Rubicon in renal cancer cells, we also checked if the complete knockout (KO) of Rubicon can further increase the efficacy of the therapeutic combination in renal cancer cells. Our observations suggest that the deletion of Rubicon can promote further induction of ROS level and increase apoptotic cell death following combination treatment. It is also associated with further downregulation of p62 and Nrf2 in RCC cells. Thus, Rubicon appears to be a potential target to induce oxidative stress in renal cancer cells following therapeutic treatments through the downregulation of p62 and Nrf2. However, in addition to the downregulation of Rubicon, it is also possible that cabozantinib + Honokiol combination treatment can partly inhibit some other tumor-promoting pathway(s) that regulate the expression of p62 and Nrf2.

The observations from our *in vivo* experiments (renal tumor xenograft model) clearly support the *in vitro* findings. Cabozantinib + Honokiol combination treatment significantly reduced the volume of renal tumors compared with controls. The expression of Rubicon in the tumor tissues was markedly downregulated; and it was associated with decreased expression of p62 and HO-1 (an effector molecule of Nrf2). These finding suggest that the combination treatment can induce oxidative stress within renal tumors through downregulation of Rubicon, which can lead to decreased p62 and Nrf2. The elevated oxidative stress following cabozantinib + Honokiol combination treatment can facilitate tumor cell death through increased apoptosis and autophagy. This is supported by our findings as the renal tumors, after combination treatment, were associated with decreased vessel density and proliferation index.

Together, the findings from this pre-clinical study suggest that cabozantinib + Honokiol combination can be a novel treatment strategy to inhibit c-Met-induced renal tumor growth and to promote oxidative stress-mediated tumor cell death. Honokiol can markedly enhance the therapeutic effectiveness of cabozantinib and inhibit key target proteins, Rubicon, p62 and Nrf2, involved in acquired therapeutic resistance. Destabilization of Nrf2 can promote oxidative stress within the tumor to facilitate cancer cell death through increased apoptosis and autophagy.

Declaration of competing interest

The authors declare that they have no known competing financial interests or personal relationships that could have appeared to influence the work reported in this paper.

Data availability

Data will be made available on request.

Acknowledgements

This work has been supported by the National Institute of Health Grants R01 CA193675 and R01 CA222355 (to S.P.). A.S. was supported by the Dana-Farber/Harvard Cancer Centre (DF/HCC), Kidney Cancer SPORE, Career Enhancement Award (CEP) 5P50CA101942-18 subaward.

References

[1] R.L. Siegel Mph, K.D. Miller, N. Sandeep, W. Mbbs, J. Dvm Ahmedin, R.L. Siegel, Cancer statistics, 2023, CA Cancer J Clin 73 (2023) 17–48, https://doi.org/10.3322/CAAC.21763.

[2] L. Schmidt, F.-M. Duh, F. Chen, T. Kishida, G. Glenn, P. Choyke, S.W. Scherer, Z. Zhuang, I. Lubensky, M. Dean, R. Allikmets, A. Chidambaram, U.R. Bergerheim, J.T. Feltis, C. Casadevall, A. Zamarron, M. Bernues, S. Richard, C.J.M. Lips, M. M. Walther, L.-C. Tsui, L. Geil, M. Lou Orcutt, T. Stackhouse, J. Lipan, L. Slife, H. Brauch, J. Decker, G. Niehans, M.D. Hughson, H. Moch, S. Storkel, M.I. Lerman, W.M. Linehan, B. Zbar, Germline and somatic mutations in the tyrosine kinase domain of the MET proto-oncogene in papillary renal carcinomas, Nat. Genet. 16 (1) (1997) 68–73, https://doi.org/10.1038/ng0597-68, 16 (1997).

[3] E. Gherardi, W. Birchmeier, C. Birchmeier, G. Vande Woude, Targeting MET in cancer: rationale and progress, Nat. Rev. Cancer 12 (2) (2012) 89–103, https://doi.org/10.1038/nrc3205, 12 (2012.

[4] P. Saraon, S. Pathmanathan, J. Snider, A. Lyakisheva, V. Wong, I. Stagljar, Receptor tyrosine kinases and cancer: oncogenic mechanisms and therapeutic approaches, Oncogene 40 (24) (2021) 4079–4093, https://doi.org/10.1038/s41388-021-01841-2, 40 (2021).

[5] Y. Sekino, J. Teishima, G. Liang, N. Hinata, Molecular mechanisms of resistance to tyrosine kinase inhibitor in clear cell renal cell carcinoma, Int. J. Urol. 29 (2022) 1419–1428, https://doi.org/10.1111/IJU.15042.

[6] P. Marona, J. Górka, J. Kotlinowski, M. Majka, J. Jura, K. Miekus, C-met as a key factor responsible for sustaining undifferentiated phenotype and therapy resistance in renal carcinomas, Cells 8 (2019), https://doi.org/10.3390/CELLS8030272.

[7] S. Chakraborty, M. Balan, E. Flynn, D. Zurakowski, T.K. Choueiri, S. Pal, Activation of c-Met in cancer cells mediates growth-promoting signals against oxidative stress through Nrf2-HO-1, Oncogenesis 8 (2) (2019) 1–12, https://doi.org/10.1038/s41389-018-0116-9, 8 (2019).

[8] M. Balan, S. Chakraborty, E. Flynn, D. Zurakowski, S. Pal, Honokiol inhibits c-Met-HO-1 tumor-promoting pathway and its cross-talk with calcineurin inhibitor-mediated renal cancer growth, Sci. Rep. 7 (1) (2017) 1–11, https://doi.org/10.1038/s41598-017-05455-1, 7 (2017).

[9] A.M.K. Choi, J. Alam, Heme Oxygenase-1: Function, Regulation, and Implication of a Novel Stress-Inducible Protein in Oxidant-Induced Lung Injury, vol. 15, 2012, pp. 9–19, https://doi.org/10.1165/AJRCMB.15.1.8679227, 10.1165/Ajrcmb.15.1.8679227.

[10] M. Nitti, S. Piras, U.M. Marinari, L. Moretta, M.A. Pronzato, A.L. Furfaro, HO-1 induction in cancer progression: a matter of cell adaptation, Antioxidants 6 (2017) 29, https://doi.org/10.3390/ANTIOX6020029, 6 (2017) 29.

[11] H.K. Na, Y.J. Surh, Oncogenic potential of Nrf2 and its principal target protein heme oxygenase-1, Free Radic. Biol. Med. 67 (2014) 353–365, https://doi.org/10.1016/J.FREERADBIOMED.2013.10.819.

[12] I. Gañán-Gómez, Y. Wei, H. Yang, M.C. Boyano-Adánez, G. García-Manero, Oncogenic functions of the transcription factor Nrf2, Free Radic. Biol. Med. 65 (2013) 750–764, https://doi.org/10.1016/J.FREERADBIOMED.2013.06.041.

[13] J. Moscat, M. Karin, M.T. Diaz-Meco, p62 in cancer: signaling adaptor beyond autophagy, Cell 167 (2016) 606–609, https://doi.org/10.1016/J.CELL.2016.09.030.

[14] Y. Katsuragi, Y. Ichimura, M. Komatsu, Regulation of the keap1–nrf2 pathway by p62/SQSTM1, Curr Opin Toxicol 1 (2016) 54–61, https://doi.org/10.1016/J.COTOX.2016.09.005.

[15] S. Adinolfi, T. Patinen, A. Jawahar Deen, S. Pitkänen, J. Härkönen, E. Kansanen, J. Küblbeck, A.L. Levonen, The KEAP1-NRF2 pathway: targets for therapy and role in cancer, Redox Biol. 63 (2023), 102726, https://doi.org/10.1016/J.REDOX.2023.102726.

[16] N. Chen, J. Debnath, Autophagy and tumorigenesis, FEBS Lett. 584 (2010) 1427–1435, https://doi.org/10.1016/J.FEBSLET.2009.12.034.

[17] N. Bata, N.D.P. Cosford, Cell survival and cell death at the intersection of autophagy and apoptosis: implications for current and future cancer therapeutics, ACS Pharmacol. Transl. Sci. 4 (2021) 1728–1746, https://doi.org/10.1021/ACSPTSCI.1C00130/ASSET/IMAGES/MEDIUM/PT1C00130_0006. GIF.

[18] N.H. Patel, S.S. Sohal, M.H. Manjili, J.C. Harrell, D.A. Gewirtz, N.H. Patel, S. S. Sohal, M. Manjili, C. J, Gewirtz, The roles of autophagy and senescence in the tumor cell response to radiation, Radiat. Res. 194 (2020) 103–115, https://doi.org/10.1667/RADE-20-00009.

[19] H. Jiang, J. Zuo, B. Li, R. Chen, K. Luo, X. Xiang, S. Lu, C. Huang, L. Liu, J. Tang, F. Gao, Drug-induced oxidative stress in cancer treatments: angel or devil? Redox Biol. 63 (2023), 102754 https://doi.org/10.1016/J.REDOX.2023.102754.

[20] B. Perillo, M. Di Donato, A. Pezone, E. Di Zazzo, P. Giovannelli, G. Galasso, G. Castoria, A. Migliaccio, ROS in cancer therapy: the bright side of the moon, Exp. Mol. Med. 52 (2) (2020) 192–203, https://doi.org/10.1038/s12276-020-0384-2, 52 (2020).
[21] J. Wu, S. Li, C. Li, L. Cui, J. Ma, Y. Hui, The non-canonical effects of heme oxygenase-1, a classical fighter against oxidative stress, Redox Biol. 47 (2021), 102170, https://doi.org/10.1016/J.REDOX.2021.102170.
[22] S. Nakamura, M. Oba, M. Suzuki, A. Takahashi, T. Yamamuro, M. Fujiwara, K. Ikenaka, S. Minami, N. Tabata, K. Yamamoto, S. Kubo, A. Tokumura, K. Akamatsu, Y. Miyazaki, T. Kawabata, M. Hamasaki, K. Fukui, K. Sango, Y. Watanabe, Y. Takabatake, T.S. Kitajima, Y. Okada, H. Mochizuki, Y. Isaka, A. Antebi, T. Yoshimori, Suppression of autophagic activity by Rubicon is a signature of aging, Nat. Commun. 10 (1) (2019) 1–11, https://doi.org/10.1038/s41467-019-08729-6, 10 (2019).
[23] S.W. Wong, P. Sil, J. Martinez, Rubicon: LC3-associated phagocytosis and beyond, FEBS J. 285 (2018) 1379–1388, https://doi.org/10.1111/FEBS.14354.
[24] J. Magné, D.R. Green, LC3-associated endocytosis and the functions of Rubicon and ATG16L1, Sci. Adv. 8 (2022), https://doi.org/10.1126/SCIADV.ABO5600/ASSET/2E688FF2-80A1-4AA4-BA90-6D00150FF446/ASSETS/IMAGES/LARGE/SCIADV.ABO5600-F4. JPG.
[25] D. Marukawa, K. Gotoh, S. Kobayashi, K. Sasaki, Y. Iwagami, D. Yamada, Y. Tomimaru, H. Akita, T. Asaoka, T. Noda, H. Takahashi, M. Tanemura, Y. Doki, H. Eguchi, Rubicon can predict prognosis in patients with pancreatic ductal adenocarcinoma after neoadjuvant chemoradiotherapy, Int. J. Clin. Oncol. 28 (2023) 576–586, https://doi.org/10.1007/S10147-023-02306-0/METRICS.
[26] A. Sabarwal, J. Wedel, K. Liu, D. Zurakowski, S. Chakraborty, E. Flynn, D. M. Briscoe, M. Balan, S. Pal, A Combination therapy using an mTOR inhibitor and Honokiol effectively induces autophagy through the modulation of AXL and Rubicon in renal cancer cells and restricts renal tumor growth following organ transplantation, Carcinogenesis 43 (2022) 360–370, https://doi.org/10.1093/CARCIN/BGAB126.
[27] H. Singh, M. Brave, J.A. Beaver, J. Cheng, S. Tang, E. Zahalka, T.R. Palmby, R. Venugopal, P. Song, Q. Liu, C. Liu, J. Yu, X.H. Chen, X. Wang, Y. Wang, P. G. Kluetz, S.R. Daniels, E.J. Papadopoulos, R. Sridhara, A.E. McKee, A. Ibrahim, G. Kim, R. Pazdur, U.S. Food and Drug Administration approval: cabozantinib for the treatment of advanced renal cell carcinoma, Clin. Cancer Res. 23 (2017) 330–335, https://doi.org/10.1158/1078-0432.CCR-16-1073/128559/AM/U-S-FOOD-AND-DRUG-ADMINISTRATION-APPROVAL.
[28] K.Y. Park, H.O. Hefti, P. Liu, K.M. Lugo-Cintrón, S.C. Kerr, D.J. Beebe, Immune cell mediated cabozantinib resistance for patients with renal cell carcinoma, Integr. Biol. 13 (2021) 259–268, https://doi.org/10.1093/INTBIO/ZYAB018.
[29] F. Koinis, P. Corn, N. Parikh, J. Song, I. Vardaki, I. Mourkioti, S.H. Lin, C. Logothetis, T. Panaretakis, G. Gallick, Resistance to MET/VEGFR2 inhibition by cabozantinib is mediated by YAP/TBX5-Dependent induction of FGFR1 in castration-resistant prostate cancer, Cancers 12 (2020) 244, https://doi.org/10.3390/CANCERS12010244, 12 (2020) 244.
[30] S.R. Lin, C.H. Chang, C.F. Hsu, M.J. Tsai, H. Cheng, M.K. Leong, P.J. Sung, J. C. Chen, C.F. Weng, Natural compounds as potential adjuvants to cancer therapy: preclinical evidence, Br. J. Pharmacol. 177 (2020) 1409–1423, https://doi.org/10.1111/bph.14816.
[31] F. Majolo, L.K. de Oliveira Becker Delwing, D.J. Marmitt, I.C. Bustamante-Filho, M. I. Goettert, Medicinal plants and bioactive natural compounds for cancer treatment: important advances for drug discovery, Phytochem. Lett. 31 (2019) 196–207, https://doi.org/10.1016/J.PHYTOL.2019.04.003.
[32] L. Rawat, V. Nayak, Ursolic acid disturbs ROS homeostasis and regulates survival-associated gene expression to induce apoptosis in intestinal cancer cells, Toxicol. Res. 10 (2021) 369–375, https://doi.org/10.1093/toxres/tfab025.
[33] A. Lewinska, D. Bednarz, J. Adamczyk-Grochala, M. Wnuk, Phytochemical-induced nucleolar stress results in the inhibition of breast cancer cell proliferation, Redox Biol. 12 (2017) 469–482, https://doi.org/10.1016/J.REDOX.2017.03.014.
[34] A. Rauf, S. Patel, M. Imran, AneelaMaalik, M.U. Arshad, F. Saeed, Y.N. Mabkhot, S. S. Al-Showiman, N. Ahmad, E. Elsharkawy, Honokiol: an anticancer lignan, Biomed. Pharmacother. 107 (2018) 555–562, https://doi.org/10.1016/J.BIOPHA.2018.08.054.
[35] Y. Hamedani, S. Chakraborty, A. Sabarwal, S. Pal, S. Bhowmick, M. Balan, Novel Honokiol-eluting PLGA-based scaffold effectively restricts the growth of renal cancer cells, PLoS One 15 (2020), e0243837, https://doi.org/10.1371/JOURNAL.PONE.0243837.
[36] A. Sabarwal, S. Chakraborty, S. Mahanta, S. Banerjee, M. Balan, S. Pal, A novel combination treatment with Honokiol and rapamycin effectively restricts c-met-induced growth of renal cancer cells, and also inhibits the expression of tumor cell PD-L1 involved in immune escape, Cancers 12 (2020) 1782, https://doi.org/10.3390/CANCERS12071782, 12 (2020) 1782.
[37] A. Sabarwal, J.C. van Rooyen, J. Caburet, M. Avgenikos, A. Dheeraj, M. Ali, D. Mishra, J.S.B. de Meester, S. Stander, W.A.L. van Otterlo, C.H. Kaschula, R. P. Singh, A novel 4′-brominated derivative of fisetin induces cell cycle arrest and apoptosis and inhibits EGFR/ERK1/2/STAT3 pathways in non-small-cell lung cancer without any adverse effects in mice, Faseb. J. 36 (2022), e22654, https://doi.org/10.1096/FJ.202200669RR.
[38] M.M. Tomayko, C.P. Reynolds, Determination of subcutaneous tumor size in athymic (nude) mice, Cancer Chemother. Pharmacol. 24 (1989) 148–154, https://doi.org/10.1007/BF00300234/METRICS.
[39] A. Ianevski, A.K. Giri, T. Aittokallio, SynergyFinder 3.0: an interactive analysis and consensus interpretation of multi-drug synergies across multiple samples, Nucleic Acids Res. 50 (2022) W739–W743, https://doi.org/10.1093/NAR/GKAC382.
[40] L. Rawat, V. Nayak, Piperlongumine induces ROS mediated apoptosis by transcriptional regulation of SMAD4/P21/P53 genes and synergizes with doxorubicin in osteosarcoma cells, Chem. Biol. Interact. 354 (2022), 109832, https://doi.org/10.1016/J.CBI.2022.109832.
[41] X. Yang, H.Y. Liao, H.H. Zhang, Roles of MET in human cancer, Clin. Chim. Acta 525 (2022) 69–83, https://doi.org/10.1016/J.CCA.2021.12.017.
[42] G.T. Gibney, S.A. Aziz, R.L. Camp, P. Conrad, B.E. Schwartz, C.R. Chen, W.K. Kelly, H.M. Kluger, c-Met is a prognostic marker and potential therapeutic target in clear cell renal cell carcinoma, Ann. Oncol. 24 (2013) 343–349, https://doi.org/10.1093/ANNONC/MDS463.
[43] L.L. Pisters, A.K. El-Naggar, W. Luo, A. Malpica, S.H. Lin, C-met proto-oncogene expression in benign and malignant human renal tissues, J. Urol. 158 (1997) 724–728, https://doi.org/10.1016/S0022-5347(01)64301-5.
[44] Z. Tang, C. Li, B. Kang, G. Gao, C. Li, Z. Zhang, GEPIA: a web server for cancer and normal gene expression profiling and interactive analyses, Nucleic Acids Res. 45 (2017) W98–W102, https://doi.org/10.1093/NAR/GKX247.
[45] D.S. Chandrashekar, S.K. Karthikeyan, P.K. Korla, H. Patel, A.R. Shovon, M. Athar, G.J. Netto, Z.S. Qin, S. Kumar, U. Manne, C.J. Crieghton, S. Varambally, UALCAN: an update to the integrated cancer data analysis platform, Neoplasia 25 (2022) 18–27, https://doi.org/10.1016/J.NEO.2022.01.001.
[46] D.S. Chandrashekar, B. Bashel, S.A.H. Balasubramanya, C.J. Creighton, I. Ponce-Rodriguez, B.V.S.K. Chakravarthi, S. Varambally, UALCAN: a portal for facilitating tumor subgroup gene expression and survival analyses, Neoplasia 19 (2017) 649–658, https://doi.org/10.1016/J.NEO.2017.05.002.
[47] J.N. Markowitz, K.M. Fancher, Cabozantinib: a multitargeted oral tyrosine kinase inhibitor, Pharmacotherapy 38 (2018) 357–369, https://doi.org/10.1002/PHAR.2076.
[48] A. Rauf, A. Olatunde, M. Imran, F.A. Alhumaydhi, A.S.M. Aljohani, S.A. Khan, M. S. Uddin, S. Mitra, T. Bin Emran, M. Khayrullin, M. Rebezov, M.A. Kamal, M. A. Shariati, Honokiol: a review of its pharmacological potential and therapeutic insights, Phytomedicine 90 (2021), 153647, https://doi.org/10.1016/J.PHYMED.2021.153647.
[49] A. Ianevski, L. He, T. Aittokallio, J. Tang, SynergyFinder: a web application for analyzing drug combination dose-response matrix data, Bioinformatics 33 (2017) 2413–2415, https://doi.org/10.1093/bioinformatics/btx162.
[50] L. Zhang, K. Wang, Y. Lei, Q. Li, E.C. Nice, C. Huang, Redox signaling: potential arbitrator of autophagy and apoptosis in therapeutic response, Free Radic. Biol. Med. 89 (2015) 452–465, https://doi.org/10.1016/J.FREERADBIOMED.2015.08.030.
[51] G. Manda, G. Isvoranu, M.V. Comanescu, A. Manea, B. Debelec Butuner, K. S. Korkmaz, The redox biology network in cancer pathophysiology and therapeutics, Redox Biol. 5 (2015) 347–357, https://doi.org/10.1016/J.REDOX.2015.06.014.
[52] P. Banerjee, A. Basu, B. Wegiel, L.E. Otterbein, K. Mizumura, M. Gasser, A. M. Waaga-Gasser, A.M. Choi, S. Pals, Heme oxygenase-1 promotes survival of renal cancer cells through modulation of apoptosis- and autophagy-regulating molecules, J. Biol. Chem. 287 (2012) 32113–32123, https://doi.org/10.1074/jbc.M112.393140.
[53] G. Tang, M. Cho, X. Wang, OncoDB: an interactive online database for analysis of gene expression and viral infection in cancer, Nucleic Acids Res. 50 (2022) D1334–D1339, https://doi.org/10.1093/NAR/GKAB970.
[54] R.K. Amaravadi, C.B. Thompson, The roles of therapy-induced autophagy and necrosis in cancer treatment, Clin. Cancer Res. 13 (2007) 7271–7279, https://doi.org/10.1158/1078-0432.CCR-07-1595.
[55] G. Recondo, J. Che, P.A. Jänne, M.M. Awad, Targeting MET dysregulation in cancer, Cancer Discov. 10 (2020) 922–934, https://doi.org/10.1158/2159-8290.CD-19-1446/333803/P/TARGETING-MET-DYSREGULATION-IN-CANCERMET-IN-CANCER.
[56] L. Poillet-Perez, G. Despouy, R. Delage-Mourroux, M. Boyer-Guittaut, Interplay between ROS and autophagy in cancer cells, from tumor initiation to cancer therapy, Redox Biol. 4 (2015) 184–192, https://doi.org/10.1016/J.REDOX.2014.12.003.
[57] L. Emdad, P. Bhoopathi, S. Talukdar, A.K. Pradhan, D. Sarkar, X.Y. Wang, S.K. Das, P.B. Fisher, Recent insights into apoptosis and toxic autophagy: the roles of MDA-7/IL-24, a multidimensional anti-cancer therapeutic, Semin. Cancer Biol. 66 (2020) 140–154, https://doi.org/10.1016/J.SEMCANCER.2019.07.013.
[58] R.K. Amaravadi, A.C. Kimmelman, J. Debnath, Targeting autophagy in cancer: recent advances and future directions, Cancer Discov. 9 (2019) 1167–1181, https://doi.org/10.1158/2159-8290.CD-19-0292/43922/P/TARGETING-AUTOPHAGY-IN-CANCER-RECENT-ADVANCES-AND.
[59] S. Chen, S.K. Rehman, W. Zhang, A. Wen, L. Yao, J. Zhang, Autophagy is a therapeutic target in anticancer drug resistance, Biochim. Biophys. Acta Rev. Canc 1806 (2010) 220–229, https://doi.org/10.1016/J.BBCAN.2010.07.003.
[60] Y. Liu, J.H. Liu, K. Chai, S.I. Tashiro, S. Onodera, T. Ikejima, Inhibition of c-Met promoted apoptosis, autophagy and loss of the mitochondrial transmembrane potential in oridonin-induced A549 lung cancer cells, J. Pharm. Pharmacol. 65 (2013) 1622–1642, https://doi.org/10.1111/JPHP.12140.
[61] Q. Sun, J. Zhang, W. Fan, K.N. Wong, X. Ding, S. Chen, Q. Zhong, The RUN domain of Rubicon is important for hVps34 binding, lipid kinase inhibition, and autophagy suppression, J. Biol. Chem. 286 (2011) 185–191, https://doi.org/10.1074/jbc.M110.126425.
[62] C. Liang, Negative regulation of autophagy, Cell Death Differ. 17 (12) (2010) 1807–1815, https://doi.org/10.1038/cdd.2010.115, 17 (2010).
[63] E. Kansanen, S.M. Kuosmanen, H. Leinonen, A.L. Levonenn, The Keap1-Nrf2 pathway: mechanisms of activation and dysregulation in cancer, Redox Biol. 1 (2013) 45–49, https://doi.org/10.1016/J.REDOX.2012.10.001.

[64] F. He, X. Ru, T. Wen, NRF2, a transcription factor for stress response and beyond, Int. J. Mol. Sci. 21 (2020) 4777, https://doi.org/10.3390/IJMS21134777, 21 (2020) 4777.
[65] A.A. Zimta, D. Cenariu, A. Irimie, L. Magdo, S.M. Nabavi, A.G. Atanasov, I. Berindan-Neagoe, The role of Nrf2 activity in cancer development and progression, Cancers 11 (2019) 1755, https://doi.org/10.3390/CANCERS11111755, 11 (2019) 1755.
[66] D. Xue, X. Zhou, J. Qiu, Emerging role of NRF2 in ROS-mediated tumor chemoresistance, Biomed. Pharmacother. 131 (2020), 110676, https://doi.org/10.1016/J.BIOPHA.2020.110676.
[67] M. Komatsu, H. Kurokawa, S. Waguri, K. Taguchi, A. Kobayashi, Y. Ichimura, Y. S. Sou, I. Ueno, A. Sakamoto, K.I. Tong, M. Kim, Y. Nishito, S.I. Iemura, T. Natsume, T. Ueno, E. Kominami, H. Motohashi, K. Tanaka, M. Yamamoto, The selective autophagy substrate p62 activates the stress responsive transcription factor Nrf2 through inactivation of Keap1, Nat. Cell Biol. 12 (3) (2010) 213–223, https://doi.org/10.1038/ncb2021, 12 (2010).